Bull Earthquake Eng (2018) 16:5647–5670
https://doi.org/10.1007/s10518-018-0403-z

ORIGINAL RESEARCH PAPER

An optimum model reference adaptive control algorithm for smart base-isolated structures

Dongbin Zhang[1] · **Peng Pan**[2,3] · **Yi Zeng**[1]

Received: 29 January 2018 / Accepted: 31 May 2018 / Published online: 5 June 2018

Abstract In structural control, appropriate control parameters and a stable closed-loop mechanism are required for a controller to achieve optimal performance, particularly in the presence of uncertain structural parameters under external excitation. In this study, an optimum model reference adaptive control (OMRAC) algorithm combining the Linear quadratic regulator method and Model Reference Adaptive Control based on Lyapunov stability is proposed. The OMRAC algorithm is implemented and applied to the response control of a base-isolated structure equipped with magneto-rheological dampers under earthquake excitations. The results from a series of numerical simulations that consider the effects of uncertainty within structural parameters are reported. The performance of the OMRAC algorithm is compared with that of other control algorithms in terms of effectiveness and stability. The results suggest that the proposed OMRAC method can successfully compensate for uncertainties in structural parameters, leading the controlled structure to adaptively track the optimal response of the reference model.

Keywords Model reference adaptive control · Linear quadratic regulator (LQR) · Lyapunov stability · Base-isolated structure · Magneto-rheological (MR) damper

1 Introduction

One of the major challenges for civil engineers is to mitigate the response of structures subjected to extreme hazards, particularly earthquakes. Over recent decades, the base-isolation system has proved to be an effective means for protecting structures and their attachments

✉ Peng Pan
panpeng@mail.tsinghua.edu.cn

[1] Department of Civil Engineering, Tsinghua University, Beijing 100084, China

[2] Key Laboratory of Civil Engineering Safety and Durability of China Education Ministry, Tsinghua University, Beijing 100084, China

[3] Institute of Internet Industry, Tsinghua University, Beijing 100084, China

from the destruction of dynamic excitations (Naeim and Kelly 1999). However, recent studies have shown that near-field ground motions characterized by long-duration pulses result in more significant displacement at the base-isolation layer (Jangid and Kelly 2001; Yang et al. 2010; Weitzmann et al. 2006). This may increase the size of the isolator and require large seismic clearance between buildings and retaining walls; in return, this increases the cost of the construction and limits the application of the isolation technology.

To improve the performance of base-isolated structures against near-field ground motions, supplemental control systems have been proposed (Barbat et al. 1995; Nagarajaiah and Narasimhan 2007; Shook et al. 2008; Dicleli 2007; Ismail 2015; Ismail et al. 2014; He et al. 2017). Passive, active, and semi-active systems are the three main categories of these strategies. Passive systems can reduce the deformation of the isolation layer during excitations. However, they cannot be adapted or tuned online, which may result in increasing the acceleration of the superstructure when large damping forces are exerted (Kelly 1999; Mazza and Vulcano 2009; Alhan and Gavin 2004). Active systems (Korkmaz 2011) are generally able to control the seismic responses of the structures using considerable external energy input, which makes them vulnerable to power failures and at the risk of destabilizing the structural behavior. Semi-active systems are more appropriate for protecting structures against earthquake excitations, because they are reliable like passive systems and adaptable like active systems. Semi-active control systems have received great attention in the past few years because of their excellent adaptability and low power requirements (Symans and Constantinou 1999; Alhan et al. 2006; Casciati et al. 2012; Basu et al. 2014; Dominguez et al. 2008; Ozbulut and Hurlebaus 2010). These systems avoid making structures unstable because they do not input energy to the structural system and only absorb or store the vibration energy. Several researchers have studied the use of semi-active devices such as magneto-rheological (MR) dampers in the base-isolated structures for the purpose of reducing the displacement response of the isolation layer without significantly increasing the acceleration response of the superstructure (Sahasrabudhe and Nagarajaiah 2005; Shi et al. 2012; Wilson and Abdullah 2010). Yoshioka et al. (2002) performed physical tests to demonstrate the effectiveness of a base-isolation system using MR dampers. Bahar et al. (2010a, b) used a new inverse model of an MR damper for the semi-active control of base-isolated structures and conducted parameter identification of large-scale magnetorheological dampers in a benchmark building.

An appropriate control algorithm is the kernel of the control systems, determining the control commands that are sent to the control devices. A number of control algorithms have been developed to control the performance of base-isolated structures equipped with active or semi-active devices. For example, decentralized bang–bang control (Feng and Shinozuka 1990), the linear quadratic regulator (LQR) (Johnson and Erkus 2007; Shi et al. 2014), clipped-optimal control (Dyke and Spencer 1996), sliding mode control (Yang et al. 1996) and fuzzy logic control (Zamani et al. 2017) have been used for semi-active control devices (Fisco and Adeli 2011; Thenozhi and Yu 2013; Etedali 2017). The majority of the above-mentioned methods do not consider the possibility of any parameter change within the controlled structure. For instance, the LQR algorithm, which ascertains the optimal control force required to minimize the response of the controlled structure, is effective and widely used in linear invariant system control, but it becomes less effective if the controlled structure is not precisely defined or if any of its parameters possess significant uncertainties (Bitaraf et al. 2012). To this end, it is essential to develop some intelligent control algorithms that are effective and stable with respect to uncertainties in structural parameters under external excitation.

Adaptive control strategies are particularly appropriate for controlling the responses of structures with parameter uncertainties, because any change in the operational conditions of the structure can be adapted by the control method (Sobel et al. 1982). Model Reference Adaptive Control (MRAC) is designed to automatically tune the controller parameters to control the response of the system. Its goal is to track the response of the controlled structure according to a reference model that exhibits the desired behavior. In recent years, MRAC has mostly been applied to automobiles and electromechanical systems (Khanna et al. 2014; Chen et al. 2016; Nguyen 2018), with a few applications to vibration control in civil engineering structures. Agarwala et al. (2000) implemented a Direct Model Reference Adaptive Control algorithm to actively control the vibration of a multi-degree-of-freedom structure. Zhang et al. (2010) and Tu et al. (2014) applied the MRAC based on Minimal Controller Synthesis (MCS) to control an active-tuned mass-damper system and an MR damper. The simulation and test results showed that the structural response could track that of the reference model successfully. However, Direct MRAC requires the controlled structure to be described accurately to satisfy Erzberger's conditions, but this is not the case with uncertain structural parameters (Zhang et al. 2010; Tu et al. 2014; Stoten and Benchoubane 1990).

The MRAC based on the Lyapunov stability theory, known as Lyapunov-MRAC, proposed in the 1960s by Shachcloth and Butchart (1965) and Parks (1966), offers improved stability and adaptation. Its application of the Lyapunov stability theory negates its requiring the controlled structure's precise information, which is particularly appropriate for controlling the structures with parameter uncertainties. Chu et al. (2010) applied the Lyapunov-MRAC to control a structure with single degree of freedom (SDOF) which possessed an active tendon device; this system's block diagram is provided in Fig. 1. In this method, a reference model with the same structural parameters but higher damping property is designed. Results showed that the Lyapunov-MRAC can stably control the structural response by tracking the response of the reference model. However, the reference model itself may not be able to consistently maintain optimal performance under different ground motions simply through an increase of its damping ratio.

Because the reference model and its output are designable and flexible, there are various possibilities for the design of this adaptive control method. In this study, by combining the MRAC based on the Lyapunov stability theory with the Linear quadratic regulator (LQR) method, an optimum model reference adaptive control (OMRAC) algorithm is developed to

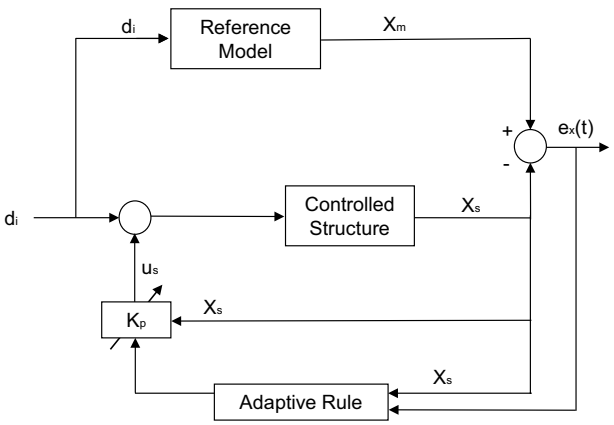

Fig. 1 Block diagram of model reference adaptive control (MRAC) in Chu et al. (2010)

control structures with uncertain parameters. The reference model is designed with a higher damping property; its mass and stiffness matrices are identical with those of the controlled structure but without its uncertainties. Additionally, the LQR controller is applied to the reference model to optimize its response, which is then used as the target for the controlled structure to track. Furthermore, the proposed adaptive law based on Lyapunov-MRAC is able to tune the parameters of the controller to compensate for the uncertainties of the controlled structure and track the response to the optimal reference output. This enables the response of a base-isolated structure with uncertainty in the base isolation or superstructure to be controlled stably and effectively under earthquake ground motions. Simulations of a base-isolated structure equipped with MR dampers under different ground motions are carried out to verify the effectiveness of the proposed OMRAC.

2 Modeling of a controlled structure with MR dampers

2.1 Dynamic model of the controlled structure

Consider an n degrees of freedom linear controlled structure subjected to earthquake acceleration $\ddot{x}_g$. The dynamic response of the controlled structure equipped with MR dampers located at certain levels of the structure is given by:

$$\mathbf{M}\ddot{x}(t) + \mathbf{C}\dot{x}(t) + \mathbf{K}x(t) = -\mathbf{M}\mathbf{I}\ddot{x}_g(t) + \mathbf{D}\mathbf{u}(t) \tag{1}$$

where $\mathbf{M}$, $\mathbf{C}$, $\mathbf{K}$ denote the $n \times n$ mass, damping, and stiffness matrices, respectively; $\mathbf{D}$ is an $n \times m$ damper location matrix and $\mathbf{I}$ is an n-dimensional identity matrix; $x(t)$, $\dot{x}(t)$, $\ddot{x}(t)$ are $n \times 1$ displacement, velocity, and acceleration vectors, respectively; and $u(t)$ is an $m \times 1$ control force vector.

Equation (1) can be written in state-space form as:

$$\dot{\mathbf{X}}(t) = \mathbf{A}\mathbf{X}(t) + \mathbf{B}\mathbf{u}(t) + \mathbf{H}\ddot{x}_g(t) \tag{2}$$

where $\mathbf{X}(t) = [x(t), \dot{x}(t)]^T$ denotes the state vector of the structural system. The system matrix, $\mathbf{A}$, and the control force location matrices, $\mathbf{B}$, and $\mathbf{H}$ are defined as follows:

$$\mathbf{A}_{2n\times 2n} = \begin{pmatrix} \mathbf{0} & \mathbf{I} \\ -\mathbf{M^{-1}K} & -\mathbf{M^{-1}C} \end{pmatrix},\ \mathbf{B}_{2n\times m} = \begin{pmatrix} \mathbf{0} \\ \mathbf{M^{-1}D} \end{pmatrix},\ \mathbf{H}_{2n\times n} = \begin{pmatrix} \mathbf{0} \\ -\mathbf{I} \end{pmatrix} \tag{3}$$

2.2 Dynamic model of the MR damper

In this study, the Bouc–Wen model is used to characterize the dynamic behavior of the MR damper, The force, f, generated by the MR damper is given as (Jansen and Dyke 2000):

$$f = c_0\dot{x} + \alpha z \tag{4}$$

$$\dot{z} = A\dot{x} - \gamma z|\dot{x}||z|^{n-1} - \beta\dot{x}|z|^n \tag{5}$$

where $\dot{x}$ is the inter-story velocity at the location of MR damper, c_0 is the viscous damping coefficient, and z describes the hysteretic behavior of the MR damper. A, β, γ and n are shape parameters employed to define the hysteresis loop of the MR damper (Kim et al. 2009). As shown in Eqs. (6) and (7), α and c_0 are both functions of the applied voltage, u_v.

$$\alpha = \alpha_a + \alpha_b u_v \tag{6}$$

$$c_0 = c_{0a} + c_{0b} u_v \tag{7}$$

$$\dot{u}_v = -\eta(u_v - v) \tag{8}$$

where α_a, α_b, c_{0a} and c_{0b} are parameters that consider the dependence of the MR damper force on applied voltage, u_v. In Eq. (8), v is the command voltage applied to the MR damper, u_v is the output voltage tuned by a first-order filter used as the applied voltage, and η is the time constant of the first order filter (Jansen and Dyke 2000).

To find the required voltage for the MR damper to produce the control force, the inverse model of the MR damper is commonly used (Bitaraf et al. 2012; Tse and Chang 2004). The voltage and force in the inverse model are as:

$$z \cong sign(\dot{x})(\frac{A}{\gamma + \beta})^{1/n}, \tag{9}$$

$$v = \frac{f - c_{0a}\dot{x} - \alpha_a z}{c_{0b}\dot{x} + \alpha_b z}, \tag{10}$$

$$\dot{u}_v = -\eta(u_v - v), \tag{11}$$

assuming that the evolutionary variable, z, can be approximated to the ultimate hysteretic strength.

Furthermore, because the applied voltage, u_v, is bounded and the MR damper can only generate passive forces, the semi-active rule for the MR damper is designed as follows:

$$u_{vf}(t) = \begin{cases} u_{v\max}, & \text{if} \quad f(t)\cdot\dot{x} < 0, u_v(t) > u_{v\max} \\ u_v(t), & \text{if} \quad f(t)\cdot\dot{x} < 0, u_v(t) \le u_{v\max} \\ 0, & \text{if} \quad f(t)\cdot\dot{x} < 0, u_v(t) \le 0 \\ 0, & \text{if} \quad f(t)\cdot\dot{x} \ge 0 \end{cases}, \tag{12}$$

where $f(t)$ is the command control force obtained from the control strategy, $u_{v\max}$ denotes the maximum applied voltage and $u_{vf}(t)$ is the applied voltage obtained from the semi-active rule.

3 Optimum model reference adaptive control algorithm

3.1 The schematic design of OMRAC

In this study, the LQR method and the MRAC based on the Lyapunov stability theory are combined. The LQR controller can be designed to optimize the reference output in the reference model, while the MRAC is designed to automatically tune the control parameters to track the response of the controlled structure with uncertainties to the reference model that exhibits the desired behavior. The block diagram of the developed OMRAC is illustrated in Fig. 2. As shown in the figure, for comparison with the Lyapunov-MRAC method in the Chu et al. (2010), a reference model with a higher damping property but lacking parameter uncertainties is also established. The input into the reference model, $\mathbf{u}_m$, is generated using the LQR method. An LQR gain matrix designed for the reference model can be obtained to minimize the reference output, $\mathbf{X}_m$, i.e., the state output of the reference model, $\mathbf{X}_m(t) = [x_m(t), \dot{x}_m(t)]^T$. For a base-isolated structure, the LQR controller should be designed to sufficiently reduce the story displacement but without significantly increasing the floor acceleration. Thus, the output,

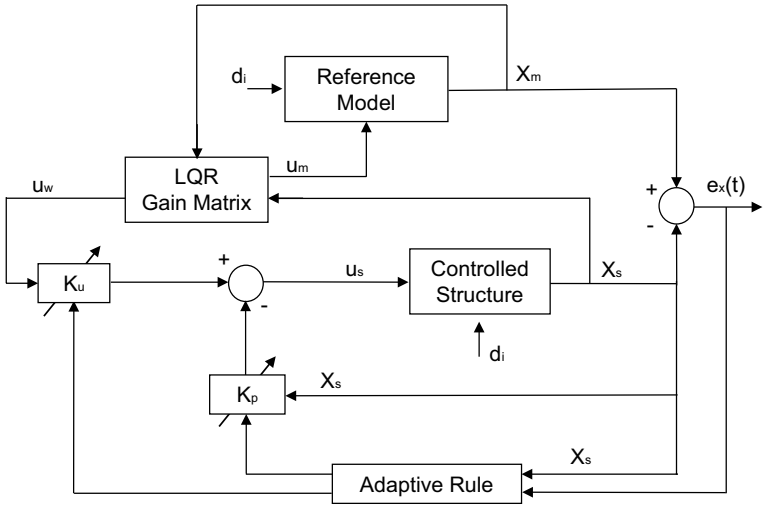

Fig. 2 Block diagram of optimum model reference adaptive control (OMRAC)

$\mathbf{X}_m$, of the reference model is the optimal signal that the controlled structure is expected to track. The controlled structure is established with parameter uncertainties, and the reference input, $\mathbf{u}_w$, is obtained using the same LQR gain matrix mentioned above. $\mathbf{X}_s$ is the state output of the controlled structure and $\mathbf{u}_s$ is the adaptive control input. d_i denotes the external excitation. $\mathbf{K}_p$ and $\mathbf{K}_u$ are two variable parameters for the adaptive controller. Note that the OMRAC algorithm is mainly designed and developed in this Section, and the behavior of MR damper is not included.

3.2 Governing equations for the OMRAC-controlled structure

Considering the earthquake excitation as an external disturbance neglected when designing the control algorithm, the governing equations for the controlled structure and the reference model are:

$$\begin{aligned} \dot{\mathbf{X}}_s(t) &= \mathbf{A}_s\mathbf{X}_s(t) + \mathbf{B}_s\mathbf{u}_s(t) \\ \mathbf{Y}_s(t) &= \mathbf{X}_s(t) \end{aligned} \tag{13}$$

$$\begin{aligned} \dot{\mathbf{X}}_m(t) &= \mathbf{A}_m\mathbf{X}_m(t) + \mathbf{B}_m\mathbf{u}_m(t) \\ \mathbf{Y}_m(t) &= \mathbf{X}_m(t) \end{aligned} \tag{14}$$

where $\mathbf{A}_s$ and $\mathbf{A}_m$ are state matrices, $\mathbf{B}_s$ and $\mathbf{B}_m$ are the input matrices, $\mathbf{X}_s$ and $\mathbf{X}_m$ are $2n \times 1$ state vectors, and $\mathbf{Y}_s$ and $\mathbf{Y}_m$ denote the output vectors of the controlled structure and the reference model, respectively. The vector, $\mathbf{u}_s$, is the $m \times 1$ control vector, and $\mathbf{u}_m$ is the $m \times 1$ reference input vector.

For the reference model, the LQR method obtains the optimal feedback gain matrix, $\mathbf{G}_m$, and optimal reference input vector, $\mathbf{u}_m$. These minimize the performance index, $\mathbf{J}$, as follows (Burl 1998):

$$\mathbf{u}_m = -\mathbf{G}_m\mathbf{X}_m \tag{15}$$

$$\mathbf{J} = \int_0^\infty (\mathbf{X}_m^T\mathbf{Q}\mathbf{X}_m + \mathbf{u}_m^T\mathbf{R}\mathbf{u}_m)dt \tag{16}$$

where $\mathbf{Q}$ and $\mathbf{R}$ are weighting matrices. $\mathbf{X}_m$ represents the state output of the reference model, i.e. displacement and velocity, and $\mathbf{u}_m$ is the control input and has influence on the acceleration output. Thus, by choosing appropriate $\mathbf{Q}$ and $\mathbf{R}$, the state output of the reference model can be minimized without significantly increasing the acceleration output under different ground motions.

3.3 Design of the adaptive feedback control law based on the Lyapunov theory

For the controlled structure, uncertainties in the structural parameters mean that the state matrix, $\mathbf{A}_S$, often cannot be described accurately. LQR is sensitive to it and, therefore, may not be able to maintain the effectiveness and stability (Bitaraf et al. 2012). Fortunately, MRAC, based on the Lyapunov stability theory, can compensate for the defects.

The OMRAC vector, $\mathbf{u}_s$, can be written as follows:

$$\mathbf{u}_s = -\mathbf{K}_p[\mathbf{e}_x(t), t]\mathbf{X}_s(t) + \mathbf{K}_u[\mathbf{e}_x(t), t]\mathbf{u}_w(t) \tag{17}$$

$$\mathbf{u}_w(t) = -\mathbf{G}_m\mathbf{X}_s(t) \tag{18}$$

$$\mathbf{e}_x(t) = \mathbf{Y}_m(t) - \mathbf{Y}_s(t) = \mathbf{X}_m(t) - \mathbf{X}_s(t) \tag{19}$$

where $\mathbf{K}_p[e_x(t), t]$ is an $m \times n$ time-variant gain matrix, $\mathbf{K}_u[e_x(t), t]$ is an $m \times m$ time-variant gain matrix, $\mathbf{u}_w$ is the reference input, $\mathbf{G}_m$ is the optimal gain matrix described above, and $\mathbf{e}_x(t)$ is the state error between the reference model and the controlled structure.

Substituting Eqs. (15), (17), and (18) into Eqs. (13) and (14), we obtain:

$$\dot{\mathbf{X}}_s(t) = \left[\mathbf{A}_s - \mathbf{B}_s\mathbf{K}_p[\mathbf{e}_x(t), t] - \mathbf{B}_s\mathbf{K}_u[\mathbf{e}_x(t), t]\mathbf{G}_m\right]\mathbf{X}_s(t) \tag{20}$$

$$\dot{\mathbf{X}}_m(t) = \left[\mathbf{A}_m - \mathbf{B}_m\mathbf{G}_m\right]\mathbf{X}_m(t) \tag{21}$$

It can be assumed that $\mathbf{K}_p^*$ and $\mathbf{K}_u^*$ exist and satisfy,

$$\begin{cases} \mathbf{A}_s - \mathbf{B}_s\mathbf{K}_p^* = \mathbf{A}_m \\ \mathbf{B}_s\mathbf{K}_u^*\mathbf{G}_m = \mathbf{B}_m\mathbf{G}_m \end{cases} \tag{22}$$

where $\mathbf{K}_p^*$ and $\mathbf{K}_u^*$ are the corresponding parameters for the controller vector $\mathbf{u}_s$ when the controlled structure matches the reference model.

In this study, Lyapunov stability theory is applied to design the model reference adaptive controller. Substituting Eqs. (20), (21), and (22) into Eq. (19), we have:

$$\begin{aligned} \dot{\mathbf{e}}_x(t) =& \dot{\mathbf{X}}_m(t) - \dot{\mathbf{X}}_s(t) \\ =& (\mathbf{A}_m - \mathbf{B}_m\mathbf{G}_m)\mathbf{e}_x(t) + (\mathbf{A}_m - \mathbf{A}_s + \mathbf{B}_s\mathbf{K}_p)\mathbf{X}_s(t) + (\mathbf{B}_s\mathbf{K}_u\mathbf{G}_m - \mathbf{B}_m\mathbf{G}_m)\mathbf{X}_s(t) \\ =& (\mathbf{A}_m - \mathbf{B}_m\mathbf{G}_m)\mathbf{e}_x(t) - \mathbf{B}_s(\mathbf{K}_p^* - \mathbf{K}_p)\mathbf{X}_s(t) - \mathbf{B}_s(\mathbf{K}_u^* - \mathbf{K}_u)\mathbf{G}_m\mathbf{X}_s(t) \\ =& (\mathbf{A}_m - \mathbf{B}_m\mathbf{G}_m)\mathbf{e}_x(t) - \mathbf{B}_s\tilde{\mathbf{K}}_p\mathbf{X}_s(t) - \mathbf{B}_s\tilde{\mathbf{K}}_u\mathbf{G}_m\mathbf{X}_s(t) \end{aligned} \tag{23}$$

where $\tilde{\mathbf{K}}_p = \mathbf{K}_p^* - \mathbf{K}_p$ and $\tilde{\mathbf{K}}_u = \mathbf{K}_u^* - \mathbf{K}_u$ are the errors in the controller parameters. Equation (23) is the governing equation of the error in the state and controller parameters, i.e. $\mathbf{e}_x(t)$, $\tilde{\mathbf{K}}_p$ and $\tilde{\mathbf{K}}_u$. Because the gain matrix $\mathbf{G}_m$ is obtained by using Linear quadratic regulator method with state matrices $\mathbf{A}_m$ and $\mathbf{B}_m$, the stability of $\mathbf{A}_m - \mathbf{B}_m\mathbf{G}_m$ can be maintained. Based on the Lyapunov Stability Theory, it means that there exist symmetrical positive definite matrices $\mathbf{P}$ and $\mathbf{Q}_m$ satisfying the Lyapunov Equation as follow:

$$(\mathbf{A}_m - \mathbf{B}_m\mathbf{G}_m)\mathbf{P}^T + \mathbf{P}(\mathbf{A}_m - \mathbf{B}_m\mathbf{G}_m) = -\mathbf{Q}_m \tag{24}$$

where $\mathbf{Q}_m$ is defined as an identity matrix.

Using the symmetrical positive definite matrix, $\mathbf{P}$, the Lyapunov function, $\mathbf{V}(t)$, can be written in terms of $\mathbf{e}_x(t)$, $\tilde{\mathbf{K}}_p$, and $\tilde{\mathbf{K}}_u$ as:

$$\begin{aligned}\mathbf{V}(t) =& \mathbf{e}_x^T(t)\mathbf{P}\mathbf{e}_x(t) + tr\{\tilde{\mathbf{K}}_p^T[\mathbf{e}_x(t),t]\boldsymbol{\Gamma}_p^{-1}\tilde{\mathbf{K}}_p[\mathbf{e}_x(t),t]\}\\ &+ tr\{\tilde{\mathbf{K}}_u^T[\mathbf{e}_x(t),t]\boldsymbol{\Gamma}_u^{-1}\tilde{\mathbf{K}}_u[\mathbf{e}_x(t),t]\}\end{aligned} \tag{25}$$

where $\boldsymbol{\Gamma}_p^{-1}$ and $\boldsymbol{\Gamma}_u^{-1}$ are symmetrical positive definite matrices of appropriate dimensions. According to the Lyapunov stability theory, if $\mathbf{V}(t)$ satisfies the following conditions, the stability condition of the system is guaranteed.

(1) $\mathbf{V}(t) > 0$ and $\mathbf{V}(t)$ is bounded.
(2) $\dot{\mathbf{V}}(t) \leq 0$.

Using conditions (1) and (2), the adaptive law of the control parameters, i.e. $\mathbf{K}_p[\mathbf{e}_x(t),t]$ and $\mathbf{K}_u[\mathbf{e}_x(t),t]$, can be designed to maintain a stable system and minimize the error between the controlled system and the reference model, i.e., $\mathbf{e}_x(t) \to 0$. A detailed proof is given in the "Appendix".

To obtain $\mathbf{K}_p[\mathbf{e}_x(t),t]$ and $\mathbf{K}_u[\mathbf{e}_x(t),t]$, their derivatives are first calculated by using Eqs. (26) and (27) at each time step, and then their values can be easily obtained by following an iterative procedure as shown in Eqs. (28) and (29).

$$\dot{\mathbf{K}}_p[\mathbf{e}_x(t),t] = -\boldsymbol{\Gamma}_p\mathbf{B}_s^T\mathbf{P}\mathbf{e}_x(t)\mathbf{X}_s^T(t) \tag{26}$$

$$\dot{\mathbf{K}}_u[\mathbf{e}_x(t),t] = \boldsymbol{\Gamma}_u\mathbf{B}_s^T\mathbf{P}\mathbf{e}_x(t)(-\mathbf{G}_m\mathbf{X}_s(t)) \tag{27}$$

$$\mathbf{K}_p^{i+1} = \mathbf{K}_p^i + dt\cdot\dot{\mathbf{K}}_p^i \tag{28}$$

$$\mathbf{K}_u^{i+1} = \mathbf{K}_u^i + dt\cdot\dot{\mathbf{K}}_u^i \tag{29}$$

In this way, the OMRAC controller given by Eq. (17) can be obtained; it is not difficult to realize in practice and will not lead to a complex computational problem. Furthermore, it can be seen that the state matrix of the controlled structure, $\mathbf{A}_S$, does not appear from Eq. (24) to (29), which means that the $\mathbf{A}_S$ is not required for the derivation of the adaptive rule. Thus, the state matrix of the controlled structure, $\mathbf{A}_S$, does not require precise information, meaning that OMRAC is effective and adaptive under uncertainties in structural parameters. Theoretically, there is no limitation in the deviation between the controlled structure and the reference model as long as they have the same dimension. However, in reality, excessive deviation require a greater degree of control force and power, making it difficult for the controlled structure to track the

response of the reference model. Furthermore, this control algorithm will not be suitable for the yielding structure with hysteretic behavior, since the Lypunov Stability Theory outlined here does not consider the nonlinear hysteretic behavior of the controlled structure. Due to these limitations of the control algorithm, for the base-isolated structure, linear elastic and viscous damping representations of the isolation system are used. And under this condition, the proposed OMRAC method will be effective, adaptive and stable.

4 Numerical study

As shown in Fig. 3, an eight-story base-isolated building, studied by Yang Yang et al. (1992, 1995), was selected to investigate the performance of the developed OMRAC controller. A lumped-mass structure with one degree of freedom per floor was used in the numerical simulations. The mass of each floor of the superstructure is 3.456×10^5 kg. Nonlinear hysteretic behavior is not considered and the stiffness of the eight floors are k_{i1} $=3.4\times10^5$, 3.2×10^5, 2.85×10^5, 2.69×10^5, 2.43×10^5, 2.07×10^5, 1.69×10^5, 1.37×10^5 kN/m for $i=1, 2,\ldots, 8$, respectively. The fundamental natural vibration period of the base-fixed superstructure is 1.2 s. The mass of the base isolation is 4.5×10^5 kg. The isolation layer consists of lead rubber bearings, and is assumed to be of equivalent linear elastic with lateral stiffness, k_b, and viscous damping, c_b, which can be derived by designing the natural vibration period of the base isolation, T_b, around 2.6–3.0 s, and using the method described in Chopra (2007) as follows, with the superstructure being assumed rigid.

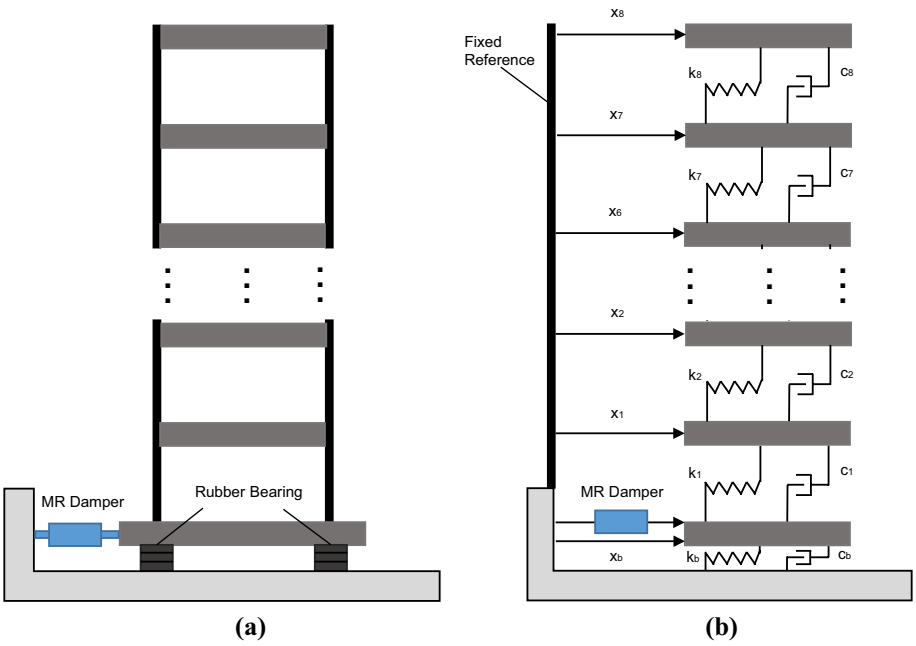

Fig. 3 Model of the smart base-isolated building as a nine degrees of freedom system. **a** Controlled structure and **b** controlled model

$$T_b = \frac{2\pi}{\omega_b}, \omega_b = \sqrt{\frac{k_b}{\sum_i m_i + m_b}}, \xi_b = \frac{c_b}{2(\sum_i m_i + m_b)\omega_b} \tag{30}$$

where ξ_b is the damping ratio of the isolation system. According to Chopra (2007), the damping ratio of the superstructure, ξ, is selected 2%. And based on the MCEER report 15-0005 (McVitty and Constantinou 2015), the effective damping of the base isolation, ξ_b, is adopted 15%. Then the lateral stiffness, k_b, of the base isolation is calculated 18,050 kN/m, and the viscous damping, c_b, can be obtained. Furthermore, the classical stiffness proportional damping matrix of the superstructure, C_s, can be obtained by using C_s=$a_1 K_s$, with a_1 chosen to achieve 2% damping in the fundamental mode, where K_s is the stiffness matrix of the superstructure (Chopra 2007; Pant et al. 2013).

In the real controlled structure, 20% degeneration of the stiffness of the base isolation, is considered as uncertain parameters, which is assumed unknown in the design of various control methods. The first two vibration periods of the controlled structure with uncertain parameters are 3.14 and 0.68 s.

In the reference model, the mass and stiffness are identical but without the uncertainties. Referring to the Chu et al. (2010), to reduce the response of the reference model and establish a better reference for the controlled model to track, the damping ratio of the superstructure, ξ_m, and that of the isolation layer, ξ_{mb}, of the reference model are enlarged to values of 0.1 and 0.2, respectively. The damping matrix of the reference model can be obtained as mentioned above. The first two vibration periods of the reference model without uncertain parameters are 2.84 and 0.67 s, respectively.

To improve the performance of the base-isolated building against earthquake excitation, an MR damper is installed in the base isolation of the structure. In the simulation, the relative parameters of the MR damper are derived and adjusted from Reference (Bitaraf et al. 2012), as demonstrated in Table 1.

Eight earthquake ground motions were applied. The peak ground accelerations of the ground motions were adjusted to 0.4 g in the numerical simulations. Figure 4 gives the acceleration spectra for the selected earthquakes. It can be observed that Taft, Hachinohe, Chi–Chi and Loma Prieta are ground motions with more long period components.

Time history analyses of the controlled base-isolated structure were conducted in MATLAB/Simulink and the explicit Runge–Kutta method was applied to solve the response history analysis. The matrices of the controlled structure and the reference model, $\mathbf{A}_S$ and $\mathbf{B}_S$, and $\mathbf{A}_m$ and $\mathbf{B}_m$, can be obtained from Eq. (3).

In the OMRAC, the weighting matrices, $\mathbf{Q}$ and $\mathbf{R}$, of the LQR method define the level of vibration and the control cost, respectively, and different weighting matrices may lead to diverse control effects. In this study, a Genetic Algorithm is used to determine the weighting

Table 1 MR damper parameters for simple Bouc–Wen model

Parameter	Value	Parameter	Value
c_{0a}	640 N/(m/s)	β	300 m^{-1}
c_{0b}	164000 N/(m/s V)	A	1.2
α_a	6.0872×10^7 N/m	n	1
α_b	16.9615×10^5 N/(m V)	η	50 s^{-1}
γ	300 m^{-1}	$u_v$max	15 V

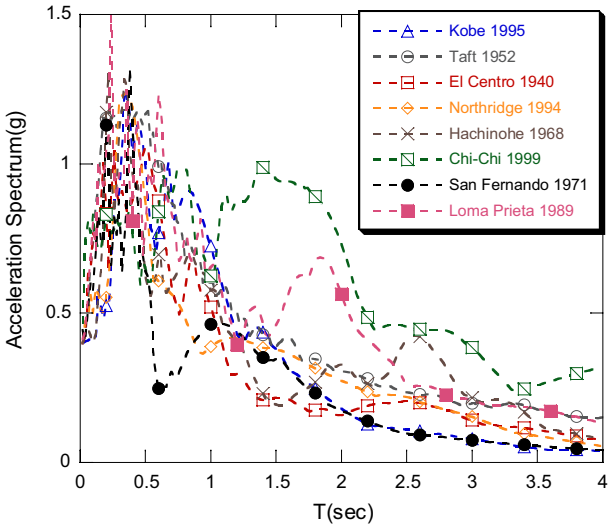

Fig. 4 Acceleration spectrum for the selected earthquakes

matrices, **Q** and **R**, of the LQR method, which is applied to optimize the response of the reference model, i.e. for the base isolated structure, sufficiently decreasing the story displacement without significantly increasing the floor acceleration. Therefore, the objective function of the Genetic Algorithm is

$$\min f = \frac{\max(disp)}{\max(disp_0)} + \frac{\max(acc)}{\max(acc_0)} \tag{31}$$

where *disp* and *acc* are the story displacement and acceleration of the controlled reference model; and $disp_0$ and acc_0 are the response of the uncontrolled reference model. By doing this, the appropriate values of **Q** and **R** can be selected for different earthquakes, i.e. $100\begin{bmatrix}\mathbf{K} & \\ & \mathbf{M}\end{bmatrix}$ and 8×10^{-5}, so that the optimal gain matrix of the LQR controller, $\mathbf{G}_m$, can be obtained. The symmetrical positive definite matrix **P** can be obtained from Eq. (24). After determining the weighting matrices, **Q** and **R**, $\mathbf{\Gamma}_p$ and $\mathbf{\Gamma}_u$ of adaptive rule can be selected. They are two definite parameters of the adaptive law and dominate the adaptive rate according to Eqs. (26) and (27). They can also be determined through the Genetic Algorithm optimization procedure, whose objective function is the deviation between the response of the controlled structure and the reference model; they are given in this example as 4×10^{13} and 3000, respectively.

Table 2 Description of control methods

Index	Method	Description
1	Uncontrolled	No controller
2	Passive control	Passive method using MR damper
3	LQR	LQR method using MR damper
4	MRAC	Designed by Lyapunov-MRAC using MR damper
5	OMARC	Combine Lyapunov-MRAC with LQR controller using MR damper

The base-isolated structure was analyzed using five different control methods provided in Table 2. The first does not use any control devices, and is designated as an uncontrolled method, the second uses a passive control method, the third uses the LQR method, the fourth employs the MRAC method developed in Chu et al. (2010), and the fifth is the proposed OMRAC method. The passive method uses the same MR damper, while its applied voltage is constant and equal to the maximum value that it can provide. The LQR controller in the LQR method is designed based on the structure without uncertain parameters, assuming that the uncertainty is unknown.

The control algorithm for Chu's et al. (2010) MRAC method, as shown in Fig. 1, is provided as follows.

$$\mathbf{u}_s = -\mathbf{K}_p[\mathbf{e}_x(t), t]\mathbf{X}_s(t) \tag{32}$$

$$\mathbf{e}_x(t) = \mathbf{X}_m(t) - \mathbf{X}_s(t) \tag{33}$$

where $\mathbf{u}_s$ is the control vector, $\mathbf{K}_p[e_x(t), t]$ is an $m \times n$ time-variant gain matrix and $\mathbf{e}_x(t)$ is the state error between the reference model and the controlled structure. There exist symmetrical positive definite matrices $\mathbf{P}$ and $\mathbf{Q}_m$ satisfying the Lyapunov Equation:

$$\mathbf{A}_m\mathbf{P}^T + \mathbf{P}\mathbf{A}_m = -\mathbf{Q}_m \tag{34}$$

where $\mathbf{A}_m$ is the state matrix for the reference model and $\mathbf{Q}_m$ is defined as an identity matrix. Then, after using the Lyapunov Stability Theory, its adaptive law is as follow.

$$\dot{\mathbf{K}}_p[\mathbf{e}_x(t), t] = -\mathbf{\Gamma}_p\mathbf{B}_s^T\mathbf{P}\mathbf{e}_x(t)\mathbf{X}_s^T(t) \tag{35}$$

where $\mathbf{\Gamma}_p$ refers to the symmetrical positive definite matrices of appropriate dimensions and, in this case, selected 4×10^{13}. Note that the reference models in the MRAC and OMARC method are designed to be identical.

Table 3 presents the maximum response for the controlled base-isolated structure under different control strategies when subject to the selected earthquakes. The maximum deformation of the base-isolation layer, $x_{b,\max}$; the maximum inter-story displacement, $d_{s\max}$; the maximum story acceleration, $\ddot{x}_{s,\max}$; and the maximum damper force, $F_{d,\max}$, are compared.

The passive method has good performance in reducing the maximum isolation displacement for all ground motions. Compared with the uncontrolled case, the reduction in the maximum isolation displacement is 10–46% for all ranges of ground motions. The maximum inter-story displacement of the superstructure is decreased by 13 and 9% for the Hachinohe and Loma Prieta motions, respectively, but increased by 73, 4, 3, 15, 1 and 18% for those at Kobe, Taft, El Centro, Northridge, Chi–Chi and San Fernando, respectively. Moreover, significant amplification of the maximum floor acceleration can be observed for most ground motions. In particular, the maximum floor acceleration increases by 78, 23, 29, 36, 35, 12 and 67% for Kobe, Taft, El Centro, Hachinohe, Northridge, Chi–Chi and San Fernando motions, respectively.

The proposed OMRAC method, it is effective in reducing the maximum displacement of the base-isolation layer for all ground motions without significantly increasing but even decreasing the maximum inter-story displacement and maximum floor acceleration. In particular, the maximum displacement of the base-isolation layer is reduced by 10–40% for all ground motions. The maximum inter-story displacement of the superstructure is decreased by 17, 9 and 9% for the Hachinohe, Chi–Chi and Loma Prieta motions and slightly increased by 11, 3, 13, and 12% for those at Kobe, Taft, Northridge and San Fernando, respectively. The maximum floor acceleration decreases by 11 and 10% for the Chi–Chi and Loma Prieta motions, respectively and increases by 13, 8, 1, 6, 14 and 28% for the Kobe, Taft, El Centro, Hachinohe, Northridge and San Fernando motions, respectively. It can be seen that the

Table 3 Maximum response of the base-isolated structure to selected earthquakes

Earthquake	Response	Uncontrolled	Passive	LQR	MRAC	OMRAC
Kobe	$x_{b,\max}$(cm)	13.42	9.35	11.20	12.07	10.34
	$d_{s\max}$(cm)	0.59	1.03	0.84	0.65	0.66
	$\ddot{x}_{s\max}$(g)	0.15	0.27	0.21	0.18	0.17
	$F_{d,\max}$(kN)		998	574	577	728
Taft	$x_{b,\max}$(cm)	27.38	19.73	22.22	24.54	21.27
	$d_{s\max}$(cm)	1.08	1.12	1.04	1.16	1.11
	$\ddot{x}_{s\max}$(g)	0.21	0.26	0.25	0.26	0.22
	$F_{d,\max}$(kN)		1472	929	1382	1398
El_Centro	$x_{b,\max}$(cm)	22.68	14.11	17.21	20.04	15.60
	$d_{s\max}$(cm)	0.95	0.98	0.95	0.97	0.95
	$\ddot{x}_{s\max}$(g)	0.18	0.23	0.20	0.19	0.18
	$F_{d,\max}$(kN)		1183	867	596	1073
Hachinohe	$x_{b,\max}$(cm)	30.01	16.13	20.81	25.05	18.18
	$d_{s\max}$(cm)	1.18	1.02	0.94	1.21	0.97
	$\ddot{x}_{s\max}$(g)	0.20	0.27	0.25	0.22	0.21
	$F_{d,\max}$(kN)		1488	939	1215	1389
Northridge	$x_{b,\max}$(cm)	22.20	16.82	18.81	20.15	18.13
	$d_{s\max}$(cm)	0.89	1.03	0.96	1.06	1.00
	$\ddot{x}_{s\max}$(g)	0.18	0.24	0.20	0.20	0.20
	$F_{d,\max}$(kN)		1636	952	1104	1075
Chi–Chi	$x_{b,\max}$(cm)	54.11	48.91	51.16	49.16	49.21
	$d_{s\max}$(cm)	2.56	2.58	2.46	2.41	2.32
	$\ddot{x}_{s\max}$(g)	0.32	0.36	0.29	0.37	0.29
	$F_{d,\max}$(kN)		2340	1855	1883	2332
San Fernando	$x_{b,\max}$(cm)	13.18	10.44	11.51	12.15	10.84
	$d_{s\max}$(cm)	0.58	0.69	0.63	0.63	0.66
	$\ddot{x}_{s\max}$(g)	0.10	0.16	0.15	0.10	0.13
	$F_{d,\max}$(kN)		1023	543	500	991
Loma Prieta	$x_{b,\max}$(cm)	26.01	16.04	19.10	21.00	17.65
	$d_{s\max}$(cm)	1.07	0.97	0.97	0.96	0.98
	$\ddot{x}_{s\max}$(g)	0.26	0.24	0.28	0.25	0.23
	$F_{d,\max}$(kN)		1334	974	1383	1349

proposed OMRAC method is similarly effective in reducing the maximum displacement of the isolation layer with the passive method, but has much better performance in the maximum inter-story displacement of the superstructure and maximum floor acceleration.

The performance of the LQR method, compared with the response of the proposed OMRAC method, is obviously less stable, in particular significantly increasing the maximum floor acceleration under the Kobe, Taft, Hachinohe and Loma Prieta motions, and less effective in reducing the maximum isolation displacement for all the ground motions. This is mainly because the LQR controller is designed without considering the uncertain parameters. Therefore, the obtained LQR controller is not appropriate for the real controlled structures.

For the MRAC method, compared with the proposed OMRAC method, it is obviously less effective in controlling the maximum isolation displacement, maximum inter-story

displacement and maximum floor acceleration, especially for the Kobe, Taft, El Centro, Hachinohe, Chi–Chi, San Fernando and Loma Prieta motions. The MRAC and OMRAC methods have the same reference model, but the OMRAC method is combined with an LQR controller to optimize the response of the reference model for all the ground motions. As a result, the performance of the OMRAC method, which can track the response of the reference model through the adaptive controller, is also improved. As a comparison, for the MRAC method, the responses of the base-isolated structure can be reduced by enlarging the damping ratio of the reference model, but are neither necessarily satisfactory nor stable, particularly for the ground motions with more long period components, e.g. the Taft, Hachinohe, Chi–Chi and Loma Prieta ground motions.

To further investigate the control effects of different control methods, the structural responses under the Kobe, San Fernando, Hachinohe and Loma Prieta ground motions are investigated. Figures 5 and 6 show the maximum story displacement and maximum floor acceleration when using different control methods, respectively.

Under the Kobe and San Fernando ground motions, the passive method, LQR and proposed OMRAC methods exhibit good performance in reducing the story displacement, while the MRAC method is less effective. For the floor acceleration, the MRAC and OMRAC both demonstrate good performance, while the passive and LQR methods obviously amplify the maximum floor acceleration. This is a defect of the passive method, while for the LQR method, if uncertain parameters exist, its performance can also be influenced and unstable.

Under the Hachinohe and Loma Prieta ground motions with more long period components, the uncontrolled structural response is obviously magnified. It can be seen that the proposed OMRAC method perform well in reducing the story displacement and floor acceleration. The MRAC method is much less effective. This is because the response of the reference model with only increasing the damping ratio is also amplified under long period ground motions. Therefore, the performance of the MRAC method cannot be maintained. Inversely, the proposed OMRAC method has increased the performance stability when incorporating the LQR controller into the reference model.

Figure 7 compares the time history responses of the controlled base-isolated structure of MRAC method and OMRAC method under the Kobe and Hachinohe records as examples. Figure 7a, b show the displacement time history of the base-isolation layer under Kobe, and Fig. 7c, d illustrate the isolation displacement time history under Hachinohe. It can be seen that both the MRAC and OMRAC are well able to track the response of the controlled structure with the output from the reference model. Compared with the MRAC method, the OMRAC method apparently exhibits improved performance in reducing the maximum isolation displacement through the ground motion. It is noted that the response of the reference model using the OMRAC method is obviously better than that of the MRAC method, especially under Hachinohe with more long period components.

Figures 8 and 9 show the time histories of the damper force and applied voltage for the MRAC method and the OMRAC method when subjected to the Kobe and Hachinohe ground motions. It can be seen that damper force of both the MRAC and the OMRAC change with the applied voltage. Under the Kobe ground motion, the OMRAC damper force is sometimes larger, especially during periods of 5–15 s. Under the Hachinohe ground motion, the maximum damper force of the MRAC is larger during periods of 25–40 s. The maximum applied voltages for the MRAC and OMRAC are all of 15 V, while the applied voltage of the OMRAC is sometimes more aggressive than that of MRAC.

Equations (17) and (26)–(29) indicate that $\mathbf{K}_p[e_x(t), t]$ and $\mathbf{K}_u[e_x(t), t]$ of the developed OMRAC vary with time to adapt to the difference between the response of

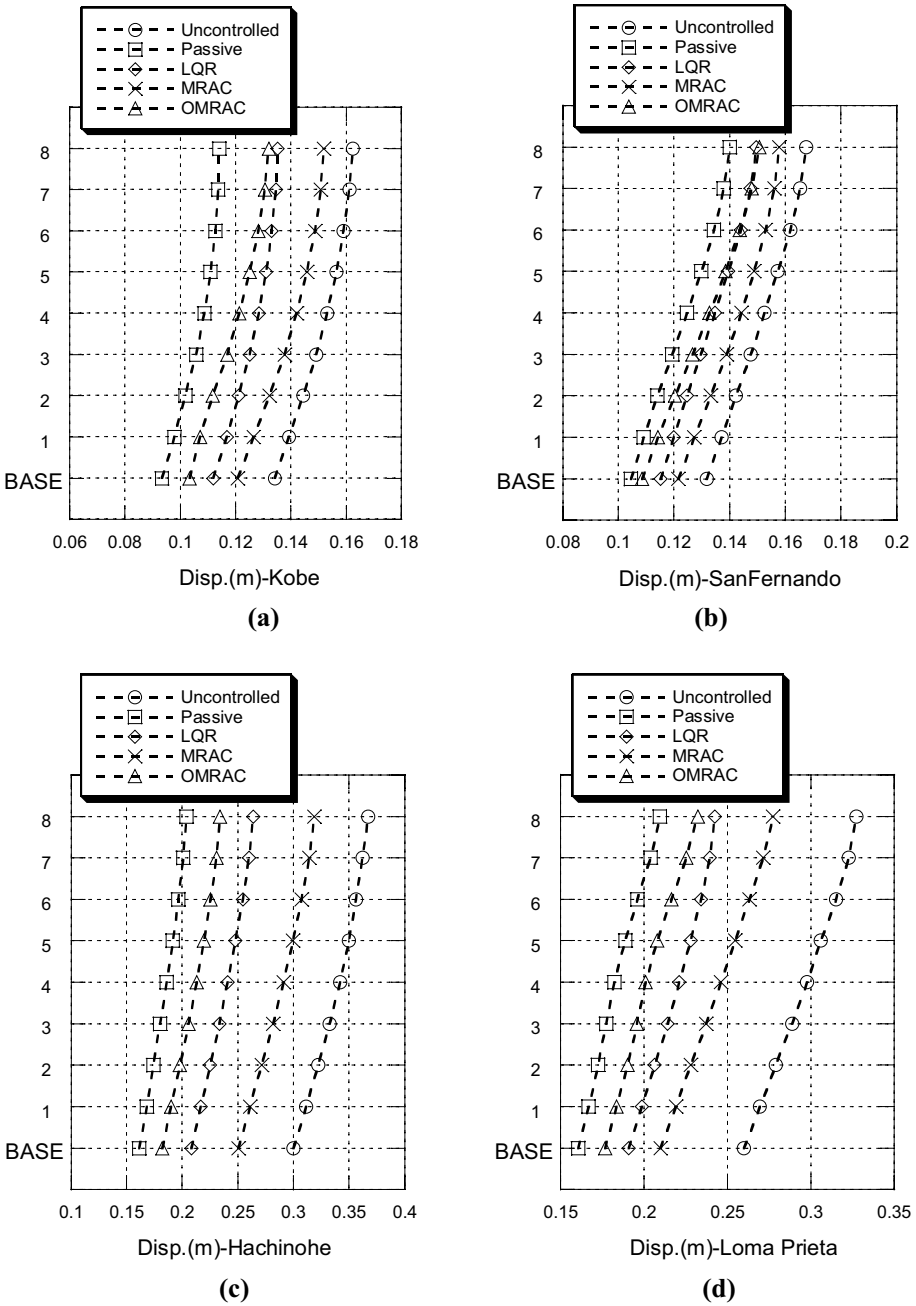

Fig. 5 Comparison of maximum story displacement. **a** Maximum story disp. of Kobe, **b** maximum story disp. of San Fernando, **c** maximum story disp. of Hachinohe and **d** maximum story disp. of Loma Prieta

the controlled structure and the target output of the reference model. In the numerical example, for the OMRAC method, $\mathbf{K}_p[e_x(t), t]$ is an 18-dimensional vector and $\mathbf{K}_u[e_x(t), t]$ is a scalar, while the MRAC method, it only has a tunable parameter

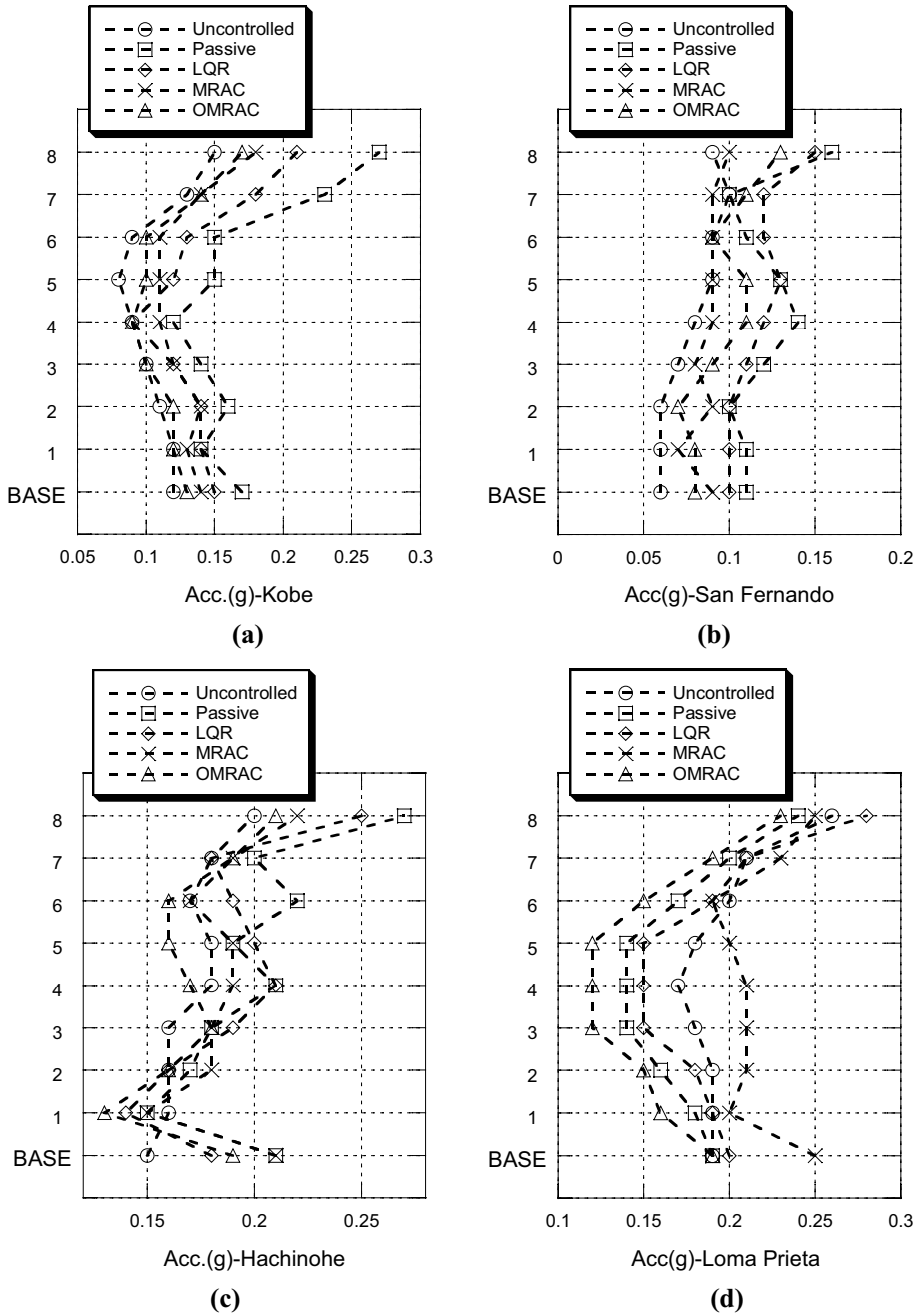

Fig. 6 Comparison of maximum floor acceleration. **a** Maximum floor acc. of Kobe, **b** maximum floor acc. of San Fernando, **c** maximum floor acc. of Hachinohe and **d** maximum floor acc. of Loma Prieta

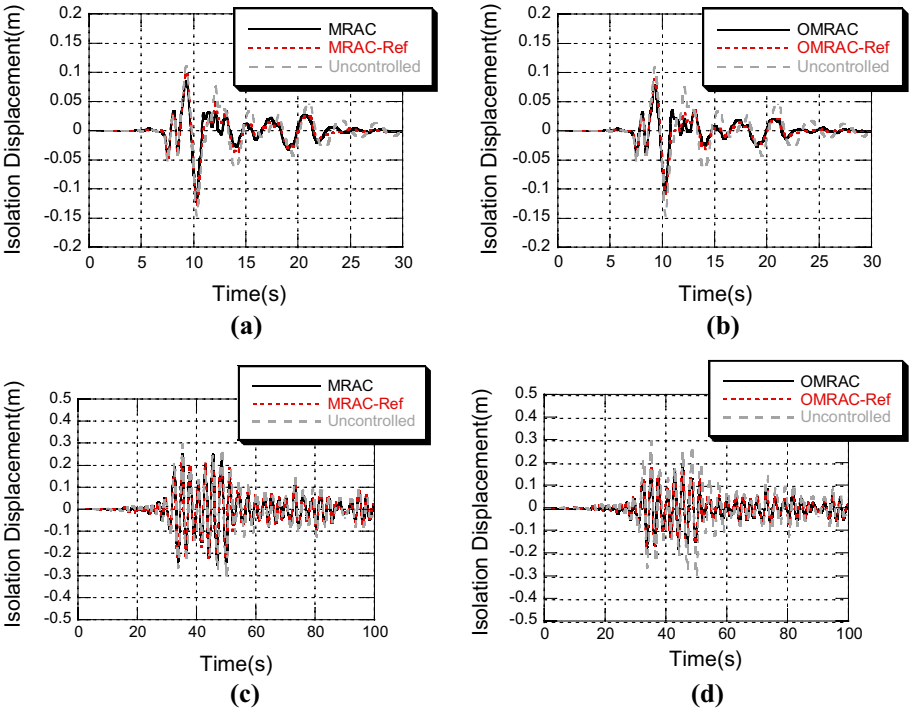

Fig. 7 Time histories of response of reference model and controlled structure under Kobe and Hachinohe. **a** Isolation displacement of MRAC under Kobe, **b** isolation displacement of OMRAC under Kobe, **c** isolation displacement of MRAC under Hachinohe and **d** isolation displacement of OMRAC under Hachinohe

$\mathbf{K}_p[e_x(t), t]$ as its 18-dimensional vector. Figure 10 shows the time histories for the variation of these tunable parameters of MRAC and OMRAC subjected to the Kobe and Hachinohe ground motions. For clarity, only the first six parameters of $\mathbf{K}_p[e_x(t), t]$ are revealed by the figures. It can be observed that the control parameters for both the MRAC and OMRAC methods can be tuned adaptively during the process. In particular, the developed OMRAC method has another parameter, $\mathbf{K}_u[e_x(t), t]$, which can also be adjusted adaptively.

In summary, it can be concluded that the passive control method performs well in reducing the maximum isolation displacement, but may induce a large amplification in the maximum inter-story displacement and maximum floor acceleration. If uncertain parameter exists, the performance of the LQR method tends to be influenced and become unstable. The MRAC method can indeed reduce the structural response but it cannot maintain its performance for diverse earthquake ground motions, especially under the ground motions with more long period components in this case. The proposed OMRAC method combines the Lyapunov-MRAC method with the LQR controller, which not only ensures an improved better and more stable response for the reference model, but also adaptively compensates for the instability of the LQR controller

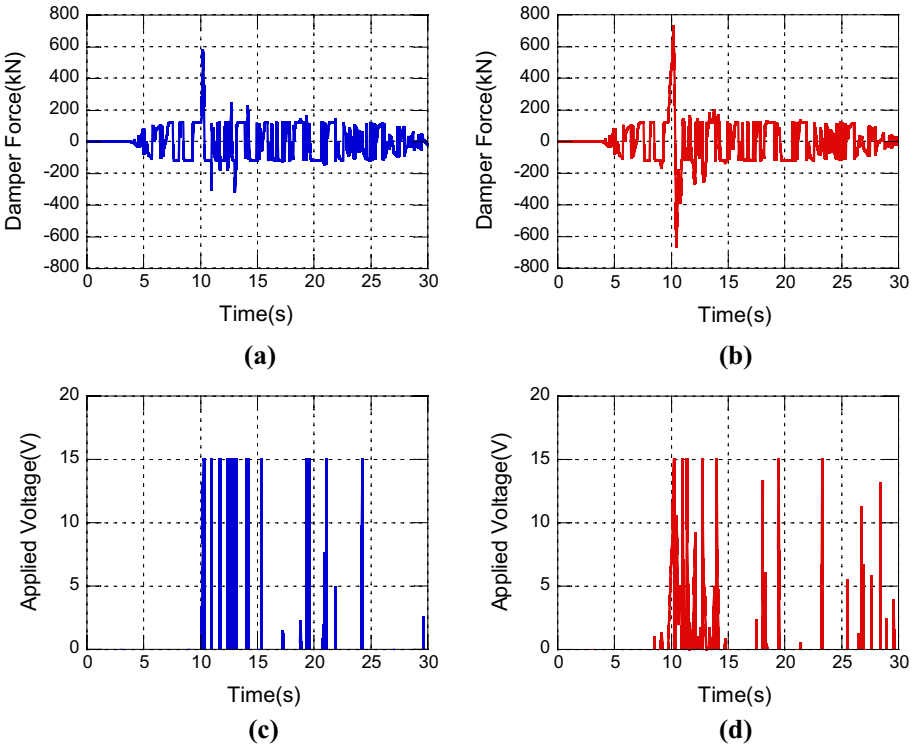

Fig. 8 Time histories of damper force and applied voltage under Kobe. **a** Damper force of MRAC, **b** damper force of OMRAC, **c** applied voltage of MRAC and **d** applied voltage of OMRAC

with uncertain parameters. Thus, it achieves good performance in reducing the maximum isolation displacement, and controlling the inter-story displacement and the floor acceleration of the superstructure under different ground motions.

5 Conclusion

An innovative adaptive control method combining Lyapunov-MRAC with the LQR method was developed to control the response of a structure in the presence of uncertain parameters. The reference model was designed with a higher damping property and LQR controller. The adaptive tuning laws of the OMRAC were developed based on the Lyapunov stability theory. The proposed OMRAC was applied to control a base-isolated structure equipped with an MR damper at the base isolation. Linear elastic and viscous damping representations of the isolation system were used. Uncertainties in structural parameters and multiple ground motions were considered. The main conclusions obtained in this study are as follows:

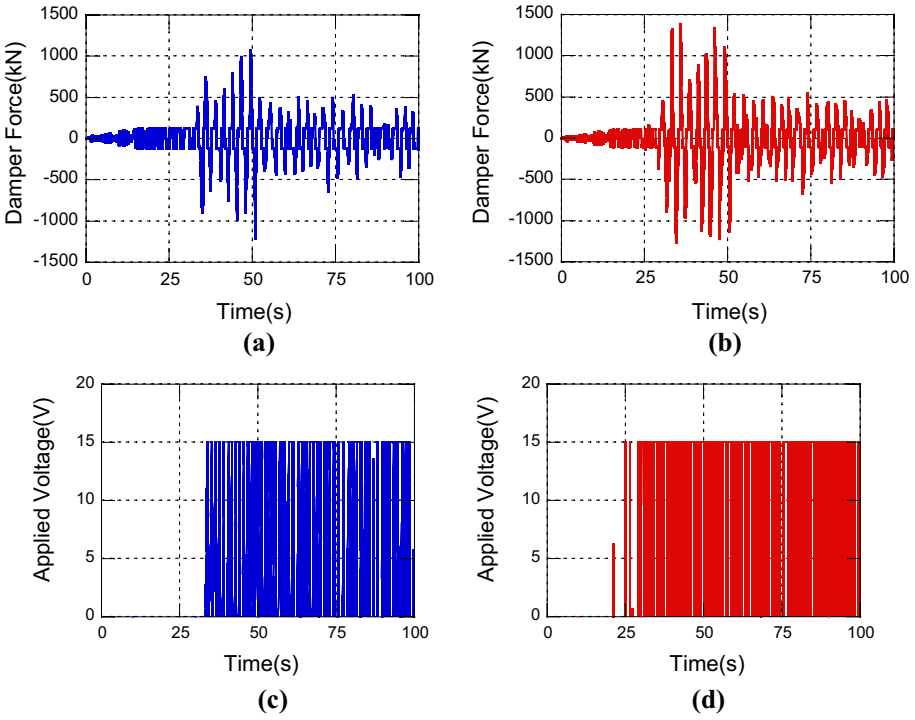

Fig. 9 Time histories of damper force and applied voltage under Hachinohe. **a** Damper force of MRAC, **b** damper force of OMRAC, **c** applied voltage of MRAC and **d** applied voltage of OMRAC

1. In the proposed OMRAC, precise information concerning the controlled structure is not required; this is applicable to structures with uncertain parameters. The optimal and stable performance of the reference model is guaranteed by the LQR controller and the adaptive tuning laws are developed based on the Lyapunov stability theory, which can tune the control parameters during the control process and compensate for uncertainties in structural parameters, making the controlled structure successfully track the response of the reference model well. Furthermore, this control algorithm will not be suitable for the yielding structure with hysteretic behavior.
2. Compared with passive method using MR damper, the OMRAC exhibits good performance in reducing the maximum displacement of the base-isolation layer, but achieves much better performance in controlling the inter-story displacement and floor acceleration of the superstructure.
3. With uncertain parameters, the performance of the LQR method is obviously less effective and unstable. The adaptive rules in the OMRAC can successfully compensate for this defection.
4. Compared with the MRAC method, the OMRAC generates a better reference model because the LQR controller is incorporated. As a result, the OMRAC method achieves better control effects in governing the isolation and inter-story displacements and floor acceleration under different ground motions.

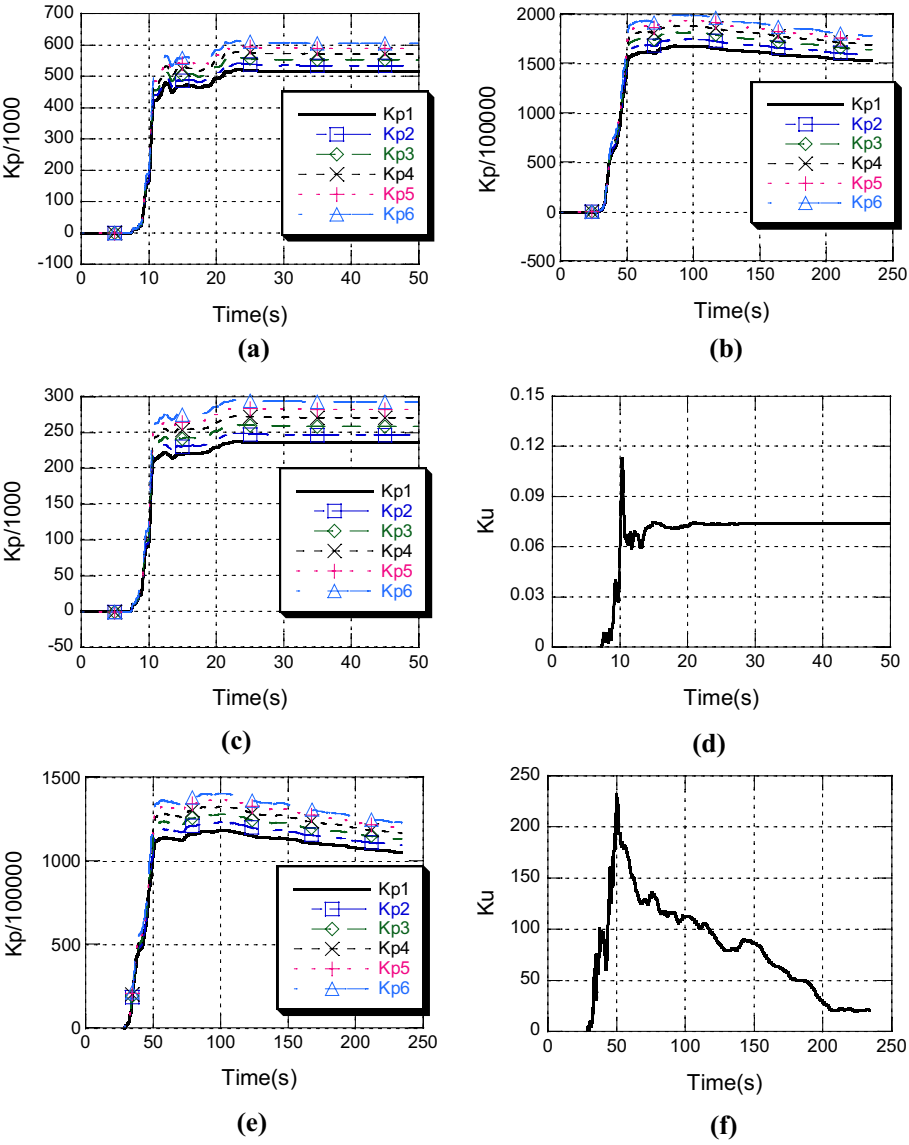

Fig. 10 Variation of control parameters of different methods. **a** Variation of $\mathbf{K}_p$ of MRAC under Kobe, **b** variation of $\mathbf{K}_p$ of MRAC under Hachinohe, **c** variation of $\mathbf{K}_p$ of OMRAC under Kobe, **d** variation of $\mathbf{K}_u$ of OMRAC under Kobe, **e** variation of $\mathbf{K}_p$ of OMRAC under Hachinohe and **f** variation of $\mathbf{K}_u$ of OMRAC under Hachinohe

Acknowledgements This work was supported by the Natural Science Foundation of China (Grant Numbers 51778342 and 51578314), Beijing Science and Technology Program (Grant Number Z161100001216015), and Institute of Internet Industry, Tsinghua University (Grant Numbers 201702001).

Appendix

The Lyapunov function $\mathbf{V}(t)$ can be written in terms of $\mathbf{e}_x(t)$, $\tilde{\mathbf{K}}_p$, and $\tilde{\mathbf{K}}_u$ as follows:

$$\begin{aligned}\mathbf{V}(t) = \mathbf{e}_x^T(t)\mathbf{P}\mathbf{e}_x(t) + tr\{\tilde{\mathbf{K}}_p^T[\mathbf{e}_x(t),t]\boldsymbol{\Gamma}_p^{-1}\tilde{\mathbf{K}}_p[\mathbf{e}_x(t),t]\}\\ + tr\{\tilde{\mathbf{K}}_u^T[\mathbf{e}_x(t),t]\boldsymbol{\Gamma}_u^{-1}\tilde{\mathbf{K}}_u[\mathbf{e}_x(t),t]\}\end{aligned} \tag{36}$$

Taking the derivative of $\mathbf{V}(t)$ with respect to time, t, and using Eq. (25), $\dot{\mathbf{V}}(t)$ can be obtained as:

$$\begin{aligned}\dot{\mathbf{V}}(t) &= \mathbf{e}_x^T(t)((\mathbf{A}_m - \mathbf{B}_m\mathbf{G}_m)\mathbf{P}^T + \mathbf{P}(\mathbf{A}_m - \mathbf{B}_m\mathbf{G}_m))\mathbf{e}_x(t)\\ &\quad - 2\mathbf{e}_x^T(t)\mathbf{P}\mathbf{B}_s\tilde{\mathbf{K}}_p[\mathbf{e}_x(t),t]\mathbf{X}_s(t) - 2\mathbf{e}_x^T(t)\mathbf{P}\mathbf{B}_s\tilde{\mathbf{K}}_u[\mathbf{e}_x(t),t]\mathbf{G}_m\mathbf{X}_s(t)\\ &\quad + tr\{\dot{\tilde{\mathbf{K}}}_p^T[\mathbf{e}_x(t),t]\boldsymbol{\Gamma}_p^{-1}\tilde{\mathbf{K}}_p[\mathbf{e}_x(t),t]\} + tr\{\dot{\tilde{\mathbf{K}}}_u^T[\mathbf{e}_x(t),t]\boldsymbol{\Gamma}_u^{-1}\tilde{\mathbf{K}}_u[\mathbf{e}_x(t),t]\}\\ &= -\mathbf{e}_x^T(t)\mathbf{Q}\mathbf{e}_x(t) - 2\mathbf{H}(t)\tilde{\mathbf{K}}_p[\mathbf{e}_x(t),t]\mathbf{X}_s(t) - 2\mathbf{H}(t)\tilde{\mathbf{K}}_u[\mathbf{e}_x(t),t]\mathbf{G}_m\mathbf{X}_s(t)\\ &\quad + tr\{\dot{\tilde{\mathbf{K}}}_p^T[\mathbf{e}_x(t),t]\boldsymbol{\Gamma}_p^{-1}\tilde{\mathbf{K}}_p[\mathbf{e}_x(t),t]\} + tr\{\dot{\tilde{\mathbf{K}}}_u^T[\mathbf{e}_x(t),t]\boldsymbol{\Gamma}_u^{-1}\tilde{\mathbf{K}}_u[\mathbf{e}_x(t),t]\}\end{aligned} \tag{37}$$

where $\mathbf{H}(t) = \mathbf{e}_x^T(t)\mathbf{P}\mathbf{B}_s$ is a $1 \times m$ vector. Because each term in Eq. (37) is one-dimensional, and using:

$$\mathbf{H}(t)\tilde{\mathbf{K}}_p[\mathbf{e}_x(t),t]\mathbf{X}_s(t) = tr\{\mathbf{X}_s(t)\mathbf{H}(t)\tilde{\mathbf{K}}_p[\mathbf{e}_x(t),t]\} \tag{38}$$

$$\mathbf{H}(t)\tilde{\mathbf{K}}_u[\mathbf{e}_x(t),t]\mathbf{G}_m\mathbf{X}_s(t) = tr\{\mathbf{G}_m\mathbf{X}_s(t)\mathbf{H}(t)\tilde{\mathbf{K}}_u[\mathbf{e}_x(t),t]\} \tag{39}$$

we can obtain:

$$\begin{aligned}\dot{\mathbf{V}}(t) &= -\mathbf{e}_x^T(t)\mathbf{Q}\mathbf{e}_x(t)\\ &\quad + tr\{\dot{\tilde{\mathbf{K}}}_p^T[\mathbf{e}_x(t),t]\boldsymbol{\Gamma}_p^{-1}\tilde{\mathbf{K}}_p[\mathbf{e}_x(t),t] - \mathbf{X}_s(t)\mathbf{e}_x^T(t)\mathbf{P}\mathbf{B}_s\tilde{\mathbf{K}}_p[\mathbf{e}_x(t),t]\}\\ &\quad + tr\{\dot{\tilde{\mathbf{K}}}_u^T[\mathbf{e}_x(t),t]\boldsymbol{\Gamma}_u^{-1}\tilde{\mathbf{K}}_u[\mathbf{e}_x(t),t] + (-\mathbf{G}_m\mathbf{X}_s(t))\mathbf{e}_x^T(t)\mathbf{P}\mathbf{B}_s\tilde{\mathbf{K}}_u[\mathbf{e}_x(t),t]\}\end{aligned} \tag{40}$$

If $\dot{\tilde{\mathbf{K}}}_p[\mathbf{e}_x(t),t]$ and $\dot{\tilde{\mathbf{K}}}_u[\mathbf{e}_x(t),t]$ are defined as:

$$\dot{\tilde{\mathbf{K}}}_p[\mathbf{e}_x(t),t] = \boldsymbol{\Gamma}_p\mathbf{B}_s^T\mathbf{P}\mathbf{e}_x(t)\mathbf{X}_s^T(t) \tag{41}$$

$$\dot{\tilde{\mathbf{K}}}_u[\mathbf{e}_x(t),t] = -\boldsymbol{\Gamma}_u\mathbf{B}_s^T\mathbf{P}\mathbf{e}_x(t)\mathbf{u}_w^T(t) = -\boldsymbol{\Gamma}_u\mathbf{B}_s^T\mathbf{P}\mathbf{e}_x(t)(-\mathbf{G}_m\mathbf{X}_s(t)) \tag{42}$$

Then,

$$\dot{\mathbf{V}}(t) = -\mathbf{e}_x^T(t)\mathbf{Q}\mathbf{e}_x(t) \le 0 \tag{43}$$

According to Eq. (23),

$$\dot{\tilde{\mathbf{K}}}_p[\mathbf{e}_x(t), t] = -\dot{\mathbf{K}}_p[\mathbf{e}_x(t), t] = \mathbf{\Gamma}_p\mathbf{B}_s^T\mathbf{P}\mathbf{e}_x(t)\mathbf{X}_s^T(t) \tag{44}$$

$$\dot{\tilde{\mathbf{K}}}_u[\mathbf{e}_x(t), t] = -\dot{\mathbf{K}}_u[\mathbf{e}_x(t), t] = -\mathbf{\Gamma}_u\mathbf{B}_s^T\mathbf{P}\mathbf{e}_x(t)(-\mathbf{G}_m\mathbf{X}_s(t)) \tag{45}$$

From Eqs. (44) and (45), we have:

$$\mathbf{K}_p[\mathbf{e}_x(t), t] = -\int_0^t \mathbf{\Gamma}_p\mathbf{B}_s^T\mathbf{P}\mathbf{e}_x(\tau)\mathbf{X}_s^T(\tau)d\tau + \mathbf{K}_p(0) \tag{46}$$

$$\begin{aligned}\mathbf{K}_u[\mathbf{e}_x(t), t] &= \int_0^t \mathbf{\Gamma}_u\mathbf{B}_s^T\mathbf{P}\mathbf{e}_x(\tau)\mathbf{u}_w^T(\tau)d\tau + \mathbf{K}_u(0)\\ &= \int_0^t \mathbf{\Gamma}_u\mathbf{B}_s^T\mathbf{P}\mathbf{e}_x(\tau)(-\mathbf{G}_m\mathbf{X}_s(\tau))d\tau + \mathbf{K}_u(0)\end{aligned} \tag{47}$$

Lemma 1 [Barbalat Lemma (Slotine and Li 1991)] *Given a function, $g(t) : R_+ \to R$, if $g(t)$ is uniformly continuous and $\lim_{t\to\infty}\int_0^t g(\tau)d\tau$ exists and is bounded, then $\lim_{t\to\infty} g(t) = 0$.*

The Lyapunov function, $\mathbf{V}(t)$, defined above, satisfies $\mathbf{V}(t) > 0$ and $\dot{\mathbf{V}}(t) \le 0$. Therefore, according to Lyapunov stability theory, the controlled system described in Eqs. (25), (44), and (45) is stable, and $\mathbf{e}_x(t)$, $\tilde{\mathbf{K}}_p$, and $\tilde{\mathbf{K}}_u$ are bounded. Furthermore, because the reference model, $\mathbf{A}_m - \mathbf{B}_m\mathbf{G}_m$, is stable and $\mathbf{X}_m(t)$ is bounded, $\mathbf{X}_s(t) = \mathbf{X}_m(t) - \mathbf{e}_x(t)$ is bounded. The control command, $\mathbf{u}_s$, is also bounded according to Eq. (17). Therefore, all of the signals in the system are bounded and stable.

According to Lemma 1, assuming that $g(t) = \dot{\mathbf{V}}(t) = -\mathbf{e}_x^T(t)\mathbf{Q}\mathbf{e}_x(t)$, we have:

$$\begin{aligned}\dot{g}(t) =& \ddot{\mathbf{V}}(t) = -2\mathbf{e}_x^T(t)\mathbf{Q}\dot{\mathbf{e}}_x(t)\\ =& -2\mathbf{e}_x^T(t)\mathbf{Q}\left\{(\mathbf{A}_m - \mathbf{B}_m\mathbf{G}_m)\mathbf{e}_x(t) - \mathbf{B}_s\tilde{\mathbf{K}}_p\mathbf{X}_s(t) - \mathbf{B}_s\tilde{\mathbf{K}}_u\mathbf{G}_m\mathbf{X}_s(t)\right\}\end{aligned} \tag{48}$$

where $\mathbf{e}_x(t)$, $\tilde{\mathbf{K}}_p$, $\tilde{\mathbf{K}}_u$, $\mathbf{X}_m(t)$, $\mathbf{X}_s(t)$ are all bounded. Therefore, $\dot{g}(t) = \ddot{\mathbf{V}}(t)$ is uniformly bounded and $g(t)$ is uniformly continuous with respect to time, t. Because $\mathbf{V}(t) > 0$ and $\dot{\mathbf{V}}(t) \le 0$, as $t \to \infty$, $\mathbf{V}(\infty)$ exists such that:

$$\lim_{t\to\infty}\int_0^t g(\tau)d\tau = \lim_{t\to\infty}\int_0^t \dot{\mathbf{V}}(t)d\tau = \mathbf{V}(\infty) - \mathbf{V}(0) \tag{49}$$

According to Lemma 1, we have:

$$\lim_{t\to\infty} g(t) = \lim_{t\to\infty}\dot{\mathbf{V}}(t) = -\lim_{t\to\infty}\mathbf{e}_x^T(t)\mathbf{Q}\mathbf{e}_x(t) = 0 \tag{50}$$

Because $\mathbf{Q}$ is a symmetrical positive definite matrix, we obtain:

$$\lim_{t\to\infty}\left\|\mathbf{e}_x(t)\right\| = 0 \tag{51}$$

References

Agarwala R, Ozcelik S, Faruqi M (2000) Active vibration control of a multi-degree-of-freedom structure by the use of direct model reference adaptive control. In: American control conference, 2000. Proceedings of the 2000. IEEE, vol 5, pp 3580–3584

Alhan C, Gavin H (2004) A parametric study of linear and non-linear passively damped seismic isolation systems for buildings. Eng Struct 26(4):485–497

Alhan C, Gavin HP, Aldemir U (2006) Optimal control: basis for performance comparison of passive and semi active isolation systems. J Eng Mech 132(7):705–713

Bahar A, Pozo F, Acho L et al (2010a) Hierarchical semi-active control of base-isolated structures using a new inverse model of magnetorheological dampers. Comput Struct 88(7):483–496

Bahar A, Pozo F, Acho L et al (2010b) Parameter identification of large-scale magnetorheological dampers in a benchmark building. Comput Struct 88(3):198–206

Barbat AH, Rodellar J, Ryan EP et al (1995) Active control of nonlinear base-isolated buildings. J Eng Mech 121(6):676–684

Basu B, Bursi OS, Casciati F et al (2014) A European Association for the control of structures joint perspective. Recent studies in civil structural control across Europe. Struct Control Health Monit 21(12):1414–1436

Bitaraf M, Hurlebaus S, Barroso LR (2012) Active and semi-active adaptive control for undamaged and damaged building structures under seismic load. Comput Aided Civil Infrastruct Eng 27(1):48–64

Burl JB (1998) Linear optimal control: H (2) and H (infinity) methods. Addison-Wesley Longman Publishing Co., Inc., Boston

Casciati F, Rodellar J, Yildirim U (2012) Active and semi-active control of structures–theory and applications: a review of recent advances. J Intell Mater Syst Struct 23(11):1181–1195

Chen Y, Wei Y, Liang S et al (2016) Indirect model reference adaptive control for a class of fractional order systems. Commun Nonlinear Sci Numer Simul 39:458–471

Chopra AK (2007) Dynamics of structures-theory and applications to earthquake engineering, 3rd edn. Prentice Hall, New Jersey

Chu SY, Lo SC, Chang MC (2010) Real-time control performance of a model-reference adaptive structural control system under earthquake excitation. Struct Control Health Monit 17(2):198–217

Dicleli M (2007) Supplemental elastic stiffness to reduce isolator displacements for seismic-isolated bridges in near-fault zones. Eng Struct 29(5):763–775

Dominguez A, Sedaghati R, Stiharu I (2008) Modeling and application of MR dampers in semi-adaptive structures. Comput Struct 86(3):407–415

Dyke SJ, Spencer BF Jr (1996) Seismic response control using multiple MR dampers. In: Proceedings of the 2nd international workshop on structural control, vol 2, pp 163–173

Etedali S (2017) A new modified independent modal space control approach toward control of seismicexcited structures. Bull Earthq Eng 15(10):4215–4243

Feng Q, Shinozuka M (1990) Use of a variable damper for hybrid control of bridge response under earthquake. In: Proceedings of the US national workshop on structural control research, USC Publ. No. CE-9013

Fisco NR, Adeli H (2011) Smart structures: part II—hybrid control systems and control strategies. Sci Iran 18(3):285–295

He J, Xu YL, Zhan S et al (2017) Structural control and health monitoring of building structures with unknown ground excitations: experimental investigation. J Sound Vib 390:23–38

Ismail M (2015) Elimination of torsion and pounding of isolated asymmetric structures under near-fault ground motions. Struct Control Health Monit 22(11):1295–1324

Ismail M, Rodellar J, Pozo F (2014) An isolation device for near-fault ground motions. Struct Control Health Monit 21(3):249–268

Jangid RS, Kelly JM (2001) Base isolation for near-fault motions. Earthq Eng Struct Dyn 30(5):691–707

Jansen LM, Dyke SJ (2000) Semiactive control strategies for MR dampers: comparative study. J Eng Mech 126(8):795–803

Johnson EA, Erkus B (2007) Dissipativity and performance analysis of smart dampers via LMI synthesis. Struct Control Health Monit 14(3):471–496

Kelly JM (1999) The role of damping in seismic isolation. Earthq Eng Struct Dyn 28(1):3–20

Khanna R, Zhang Q, Stanchina WE et al (2014) Maximum power point tracking using model reference adaptive control. IEEE Trans Power Electron 29(3):1490–1499

Kim Y, Langari R, Hurlebaus S (2009) Semi-active nonlinear control of a building with a magnetorheological damper system. Mech Syst Signal Process 23(2):300–315

Korkmaz S (2011) A review of active structural control: challenges for engineering informatics. Comput Struct 89(23):2113–2132
Mazza F, Vulcano A (2009) Nonlinear response of RC framed buildings with isolation and supplemental damping at the base subjected to near-fault earthquakes. J Earthq Eng 13(5):690–715
McVitty WJ, Constantinou MC (2015) Property modification factors for seismic isolators: design guidance for buildings. MCEER report, p 15-0005
Naeim F, Kelly JM (1999) Design of seismic isolated structures: from theory to practice. Wiley, New York
Nagarajaiah S, Narasimhan S (2007) Seismic control of smart base isolated buildings with new semi-active variable damper. Earthq Eng Struct Dyn 36(6):729–749
Nguyen NT (2018) Model-reference adaptive control. Springer, Cham, pp 83–123
Ozbulut OE, Hurlebaus S (2010) Fuzzy control of piezoelectric friction dampers for seismic protection of smart base isolated buildings. Bull Earthq Eng 8(6):1435–1455
Pant DR, Wijeyewickrema AC, ElGawady MA (2013) Appropriate viscous damping for nonlinear time-history analysis of base-isolated reinforced concrete buildings. Earthq Eng Struct Dyn 42(15):2321–2339
Parks PC (1966) Liapunov redesign of model reference adaptive control systems. IEEE Trans Autom Control 11(3):362–367
Sahasrabudhe S, Nagarajaiah S (2005) Experimental study of sliding base-isolated buildings with magnetorheological dampers in near-fault earthquakes. J Struct Eng 131(7):1025–1034
Shachcloth B, Butchart RL (1965) Synthesis of model reference adaptive control systems by Lyapunov's second methods. IFAC Aymposium, Jeddinglon
Shi Y, Becker T, Kurata M et al (2012) Design of a PI controller for MR dampers using damper force feedback. In: Proceeding of the first international symposium on earthquake engineering, pp 311–316
Shi Y, Becker TC, Furukawa S et al (2014) LQR control with frequency-dependent scheduled gain for a semi-active floor isolation system. Earthq Eng Struct Dyn 43(9):1265–1284
Shook DA, Roschke PN, Ozbulut OE (2008) Superelastic semi-active damping of a base-isolated structure. Struct Control Health Monit 15(5):746–768
Slotine JJE, Li W (1991) Applied nonlinear control. Prentice-Hall, Englewood Cliffs
Sobel K, Kaufman H, Mabius L (1982) Implicit adaptive control for a class of MIMO systems. IEEE Trans Aerosp Electron Syst 5:576–590
Stoten DP, Benchoubane H (1990) Empirical studies of an MRAC algorithm with minimal controller synthesis. Int J Control 51(4):823–849
Symans MD, Constantinou MC (1999) Semi-active control systems for seismic protection of structures: a state-of-the-art review. Eng Struct 21(6):469–487
Thenozhi S, Yu W (2013) Advances in modeling and vibration control of building structures. Annu Rev Control 37(2):346–364
Tse T, Chang CC (2004) Shear-mode rotary magnetorheological damper for small-scale structural control experiments. J Struct Eng 130(6):904–911
Tu J, Lin X, Tu B et al (2014) Simulation and experimental tests on active mass damper control system based on model reference adaptive control algorithm. J Sound Vib 333(20):4826–4842
Weitzmann R, Ohsaki M, Nakashima M (2006) Simplified methods for design of base-isolated structures in the long-period high-damping range. Earthq Eng Struct Dyn 35(4):497–515
Wilson CMD, Abdullah MM (2010) Structural vibration reduction using self-tuning fuzzy control of magnetorheological dampers. Bull Earthq Eng 8(4):1037–1054
Yang JN, Li Z, Danielians A et al (1992) Aseismic hybrid control of nonlinear and hysteretic structures I. J Eng Mech 118(7):1423–1440
Yang JN, Wu JC, Agrawal AK (1995) Sliding mode control for nonlinear and hysteretic structures. J Eng Mech 121(12):1330–1339
Yang JN, Wu JC, Reinhorn AM et al (1996) Control of sliding-isolated buildings using sliding-mode control. J Struct Eng 122(2):179–186
Yang TY, Konstantinidis D, Kelly JM (2010) The influence of isolator hysteresis on equipment performance in seismic isolated buildings. Earthq Spectra 26(1):275–293
Yoshioka H, Ramallo JC, Spencer BF Jr (2002) "Smart" base isolation strategies employing magnetorheological dampers. J Eng Mech 128(5):540–551
Zamani AA, Tavakoli S, Etedali S et al (2017) Online tuning of fractional order fuzzy PID controller in smart seismic isolated structures. Bull Earthq Eng. https://doi.org/10.1007/s10518-017-0294-4
Zhang K, Zhou L, Wang G (2010) Minimal control synthesis algorithm in structural vibration control. J Huazhong Univ Sci Technol (Urban Sci Ed) 3:018